Electron confinement and optical enhancement in Si/SiO$_2$ superlattices

Pierre Carrier,[1] Laurent J. Lewis,[1,*] M. W. C. Dharma-wardana[2]

[1]*Département de Physique et Groupe de Recherche en Physique et Technologie des Couches Minces (GCM), Université de Montréal, Case Postale 6128, Succursale Centre-Ville, Montréal, Québec, Canada H3C 3J7*

[2]*Institute for Microstructural Sciences, National Research Council, Ottawa, Canada K1A 0R6*

We have performed first-principles calculations of Si/SiO$_2$ superlattices in order to examine their electronic states, confinement, and optical transitions, using linearized-augmented-plane-wave techniques and density-functional theory. Two atomic models having fairly simple interface structure are considered. They differ in the way dangling bonds at interfaces are satisfied. The real and imaginary parts of the dielectric function are calculated at the Fermi-golden-rule level and used to estimate the absorption coefficients. Confinement is demonstrated by the dispersionless character of the electronic band structures in the growth direction. Optical enhancement is shown to exist by comparing the direct and indirect transitions in the band structures with the related transitions in bulk Si. The role played by the interface on the optical properties is assessed by comparing the absorption coefficients from the two models.

I. INTRODUCTION

Informatics and telecommunications are the driving forces behind the development of new photonic devices.[1] Such devices can be assembled from a wide variety of materials; among these, silicon is probably the most prevalent, although it suffers from having an indirect band gap. Direct band-gap materials such as GaAs, InP, and many-other III-V and II-VI semiconductors, are efficient electron-photon energy converters. However, they are costly for large-scale applications, and would be less interesting if full Si-based photonics were possible. These considerations have lead to considerable efforts towards the development of new types of Si-based materials having direct energy gap in the visible (viz. 1.5 to 3 eV),[2] suitable for photodiodes and lasers, as well as solar-cell applications.

The simultaneous discovery by Canham[3] and Lehmann and Gösele[4] of intense luminescence in porous silicon (π-Si) has opened up new horizons for Si-based materials. π-Si can be regarded as consisting of long and thin nanowires,[5] forcing the electronic states to be confined within the finite dimension of the nanostructures. The shift of the luminescence spectrum towards the blue with decreasing nanowire size[3] suggests that the confinement of the electronic states might be responsible for the visible luminescence. Unfortunately, most forms of π-Si are unstable, lasting only a few hours before a strong decrease of the luminescence efficiency is observed. This instability has sometimes been attributed to the volatile Si-H bonds at the surface.[4] Annealing under nitrogen and oxygen has been suggested as a means of stabilizing the structures. However, the annealed material has weaker luminescence than the parent π-Si. Layered polysilanes (Si$_{6n}$H$_6$) also exhibit optical properties similar to π-Si. Uehara and Tse[6] have performed first-principles calculations of layered polysilanes structures and showed that porous Si may be akin to thin Si$_6$H$_6$ sheets.

As perhaps a more promising avenue, confinement can also be achieved in superlattices (SLs) – or quantum wells – as well as quantum wires and quantum dots. Lu, Lockwood, and Baribeau have reported enhanced luminescence in the visible part of the spectrum of Si/SiO$_2$ SLs fabricated by molecular-beam epitaxy (MBE),[7] and a blue shift was observed when the thickness of the Si layers was reduced from 6 to 2 nm. In contrast to π-Si, Si/SiO$_2$ SLs present the advantage of being stable, with no significant decrease of the luminescence observed with time.

Motivated by these promising experimental observations, and to provide insight into the microscopic physics associated with the luminescence efficiency of SL-based devices, we undertook a detailed, first-principles investigation of the electronic and optical properties of Si/SiO$_2$ SLs. Silicon and SiO$_2$ are both already standard components of metal-oxide-semiconductor field-effect transistor and other devices. SiO$_2$, which is an insulator, has an energy gap of ~ 9 eV while Si has an indirect gap of ~ 1.1 eV. Thus, the electrons are strongly confined by the SiO$_2$ barriers within the silicon quantum wells. Luminescence, however, is not determined solely by confinement since the magnitude of the oscillator strength and nature of the energy gap are even more important.

In this work, we examine the luminescence properties of Si/SiO$_2$ SLs using model structures and first-principles methodology. Transmission electron microscopy reveals that in Si/SiO$_2$ SLs, both Si and SiO$_2$ layers are amorphous.[7] Amorphous structures are, however, not easily amenable to quantum calculations. Here, we assume crystalline phases for both the Si and SiO$_2$ slabs. This is further motivated by the need to study simple ideal systems as benchmarks, and in particular to determine how differences in the interfaces affect the optical properties. We also note that crystalline Si-based SLs have very recently been fabricated.[8]

Two simple-model structures for Si/SiO$_2$ SLs are considered: (i) The double-bonded model (DBM) of Herman and Batra,[9] shown in Fig. 1(a); here the Si and SiO$_2$ layers are arranged so as to minimize the lattice mismatch and have relatively high symmetry, and the dangling bonds at the interfaces are saturated by the addition of a single double-bonded oxygen atom. (ii) A bridge-oxygen model (BOM),

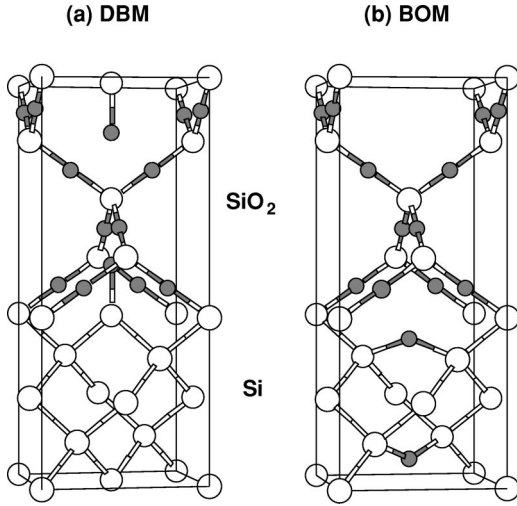**(a) DBM**   **(b) BOM**

SiO$_2$

Si

FIG. 1. The two model structures considered in the present study: (a) the DBM, which contains 23 atoms (13 Si and 10 O), and (b) the BOM, which contains 21 atoms (11 Si and 10 O atoms). Both unit cells are rectangular, of size 5.43×5.43×13.11 Å^3. The two models differ only by their Si-SiO$_2$ interface.

introduced by Tit and Dharma-wardana,[10] shown in Fig. 1(b); here the interface dangling bonds are saturated by adding an oxygen atom to bridge two Si bonds. Full details of the models are given in Sec. II A.

The electronic properties of both the DBM and the BOM have been studied within an empirical tight-binding (TB) framework by Tit and Dharma-wardana,[11] who observed the bands along the high-symmetry lines of the Brillouin zone (BZ) parallel to the k_z axis to be essentially dispersionless, in agreement with the present calculations. However, the band gaps were found to be direct in both the models, in contradiction with the *ab initio* results. The present calculations also provide more precise values for the valence-band offsets (VBO) — the difference in energy between the valence-band maximum (VBM) of the two materials constituting the SL.[12] Indeed, it was found that appropriate values of the VBO are 0.0 eV for the DBM and 1.0 eV for the BOM, while this was set to 3.75 eV in the TB calculations. The TB band gaps, however, remain direct even if the new VBO is used.

The DBM has been studied from first principles by Punkkinen *et al.*[13] using a full-potential linear-muffin-tin orbital approach. However, no other interface structure was examined and thus the effect of changing the interface could not be assessed; further, the optical properties were not calculated. Kageshima and Shiraishi have also used first-principles methods to examine different models for the Si-SiO interface in oxide-covered Si slabs,[14] but the SL geometry was not examined. Their calculations indicate that the interface plays an important role in the light-emitting properties of the system and that, in particular, interfacial Si-OH bonds are possibly related to the observed luminescence. Here we present results for the electronic structure, the dielectric function, and the absorption coefficient of both the DBM and the BOM, and focus on a comparison between the two models.

II. COMPUTATIONAL DETAILS

A. Model structures

SLs can be fabricated by MBE.[15] A major advantage of this technique, as compared to others, is that it gives sharper interfaces. In the case of Si/SiO$_2$ SLs, Lu, Lockwood, and Baribeau[7] report an interface thickness of about 0.5 nm, while the thickness of the SiO$_2$ and Si layers vary between 2 and 6 nm. The interfaces that define the transition from the Si to the SiO$_2$ region are taken to consist of two atomic planes in the exploratory models studied here.

The model Si/SiO$_2$ SL structures are constructed from alternating layers of crystalline (diamond) silicon and crystalline SiO$_2$ in the ideal β-cristobalite structure, viz. with a Si-O-Si bond angle of 180° (space group Fd$\bar{3}$m). The (experimental) lattice constants are 5.43 and 7.16 Å, respectively, with therefore a lattice mismatch of 32%. The mismatch can be reduced to less than 7% by rotating the Si unit cell by an angle of $\pi/4$ so that the diagonal of the Si-diamond structure fits, approximately, the cubic edge of the β-cristobalite unit cell. The superposition of the Si and SiO$_2$ layers gives rise to dangling bonds on some of the interface Si atoms. These can be satisfied in different ways. In the DBM, this is done by adding a single O atom onto one of the Si atoms. The resulting unit cell has 23 atoms [cf. Fig. 1(a)] and dimensions 5.43 Å in the x-y plane and 5.43×(1 + $\sqrt{2}$)=13.11 Å in the z (growth) direction. In this model, the Si-Si and Si-O distances, 2.35 and 1.66 Å, respectively, are realistic, but the double-bonded oxygen Si=O is not found in naturally occuring silicates. In the BOM, Fig. 1(b), an oxygen atom saturates two dangling bonds provided by two different Si atoms; this model contains 21 atoms. Here the Si-O-Si angle is the usual 144° and the length of the Si-O bonds at the interface is 2.02 Å, i.e., somewhat longer than found in nature. No energy relaxation of the models has been carried out. As will be discussed in Sec. III B, we found gap states to be present in the BOM; in order to understand this, we investigated two other variants of the BOM, having Si-O-Si angles of 109° and 158°, respectively.

The Brillouin zone for the SL, along with that for c-Si, is depicted in Fig. 2. The principal symmetry axes are indicated: the Z-Γ, X-R, and M-A directions correspond to possible growth directions where confinement is expected to occur, as discussed below.

In Si/SiO$_2$ SLs, the electrons in Si are confined by the SiO$_2$ layers. This implies the existence of an interface region that has to be defined in atomistic detail. An appropriate definition of the interface is provided by "suboxide," or partially oxidized, Si atoms.[16,17] In the models presented here, only suboxide Si atoms bonded to one or two O atoms are present. From Figs. 1(a) and 1(b), one sees that both models possess four suboxide Si layers, with three bulklike Si planes in the DBM and only one in the BOM. The Si layers in the BOM are thus more strongly confined, and interface effects will prevail in determining the electronic and optical properties of this model. It is known from experiment that increased confinement results in a blue shift of the absorption;[7]
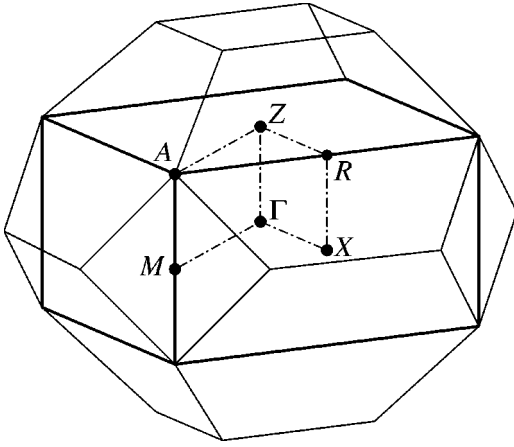
FIG. 2. Brillouin zone for the SL compared to that for the diamond structure. The principal axes of symmetry used in the electronic-structures calculations are also shown.

higher-energy gaps are thus expected in the BOM as compared to the DBM. (See also the discussions in Sec. III, as well as in Table I).

B. First-principles calculations

The electronic-structure calculations were carried out with the WIEN97 code,[18] which uses the all-electron, full-potential, linearized-augmented-plane-wave method,[19] within the framework of density-functional theory[20,21] (DFT) in the local-density approximation (LDA).[22] Thus, the core states in the (spherical) atomic region are described using an atomic basis, while the delocalized states in the interstitial region are expanded in plane waves that are correctly formulated to account for the core region. The Kohn-Sham (KS) basis inside the atomic spheres is expressed as an angular-momentum expansion:

TABLE I. Possible (LDA-DFT) transition energies (in eV) for the two models (DBM and BOM with Si-O-Si interfacial angle of 144°). CB1, CB2, and VB refer to the first and second conduction band, and the valence band, respectively. For the DBM, $\Gamma X/2$ designates the conduction band minimum, which lies approximately half-way between Γ and X points (cf. Fig. 3). The lowest direct and indirect transitions are listed; the energy gaps, which are indirect, are indicated in boldface. For the BOM, CB1 can be viewed as a gap state (see text), and the "true" LDA gap is therefore 1.49 eV; for the DBM, this gap state is absent, i.e., CB1 is the true lowest band, and the LDA gap is 0.81 eV.

	BOM		DBM	
	X	Z	Γ	$\Gamma X/2$
CB2	2.1870	1.4932		
CB1	1.7447	0.0143	0.9781	0.8050
VB	0.0000	−0.3754	0.0000	−0.0369
CB2-VB dir.	2.1870	1.8686		
CB2-VB ind.	CB2$_Z$-VB$_X$: **1.4932**			
CB1-VB dir.	1.7447	0.3897	0.9781	0.8419
CB1-VB ind.	CB1$_Z$-VB$_X$: **0.0143**		CB1$_{\Gamma X/2}$-VB$_\Gamma$: **0.8050**	

$$\psi(\vec{k}_n,\vec{r})=\sum_{l,m}\left[A_{lm}^n u_l(r,E_l)+B_{lm}^n\frac{\partial u_l}{\partial E}\bigg|_{E=E_l}\right]Y_{lm}(\hat{r}).$$

Here the energy E_l is calculated and fixed at the first cycle of the self-consistent-field calculation. The KS equations are solved for a grid of $\vec{k}$ points as discussed below.

The integration of the radial secular equations was performed on a radial mesh containing 581 points. The radius of the spheres for silicon and oxygen atoms were set at 0.87 and 0.79 Å , respectively, and an energy cutoff of -7.1 Ry was used for separating core from valence electrons. This generated 11 149 plane waves and the matrix size for the eigenvalue problem contained 5581 elements. These two parameters correspond to an angular momentum cutoff of 7.5 Ry (see Singh[19] for further details), a value that ensures proper energy convergence of the solution.

The DBM has nine nonequivalent atoms while the BOM has eight. The irreducible wedge of the Brillouin zone is obtained after four-symmetry operations, which reduces considerably the computational load. The supercell in the z direction being three times longer than in the x or y directions, only 181 $\vec{k}$ points were necessary to achieve convergence of the electronic energies. However, in order to ensure convergence of the wave functions needed to set up the optical matrix, the density of $\vec{k}$ points had to be doubled. Integration of the Brillouin zone was performed using the tetrahedron method and Broyden density mixing. The self-consistent calculations were performed in parallel mode (using eight processors) on a Silicon Graphics Origin 2000 computer system. About ten cycles were necessary to get convergence of the energy to about 10^{-4} Ry.

III. RESULTS AND DISCUSSION

A. Band structures

The electronic band structures along the high-symmetry axes of the tetragonal Brillouin zone (cf. Fig. 2) for the two models are plotted in Fig. 3, together with the densities of states (DOS). For the BOM, unless otherwise noted, the interfacial Si-O-Si angle is the normal 144°. The confinement in the z direction can already be inferred from the essentially dispersionless character of the bands along the three symmetry axes that are parallel to the axis of the SL, namely, X-R, Z-Γ, and M-A axis; this was also observed by Punkkinen et al.[13] Thus, optical transitions between bands lying in the growth direction are favored by the confinement.

The DOS of the two models differ strongly in the region of the gap, with an isolated conduction band clearly visible in the gap of the BOM that is absent in the DBM. The only difference between the two models lies in the way that the interfacial dangling bonds are fixed. The gap state in the BOM is thus connected to the bridge-bonded Si atom. The results, evidently, are sensitive to the way that the interface is formed, either in experiment, or in a theoretical model. This question will be discussed in more detail in Sec. III B.

The effect of the confinement in both models is clearly visible from the DOS. If we ignore the gap state in the BOM for the moment (but see below), the DOS at the Fermi level
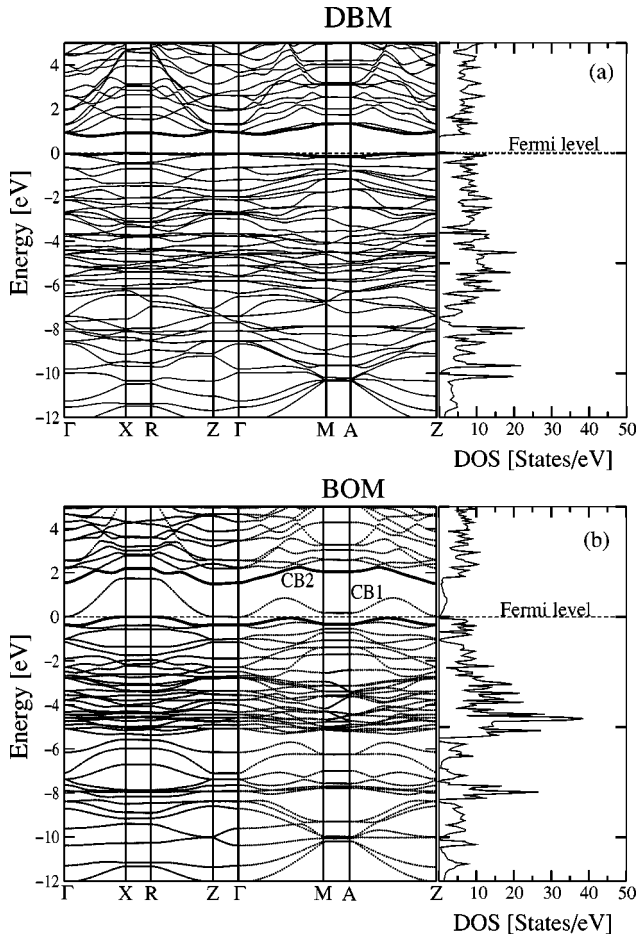
FIG. 3. Band structure and DOS for (a) the DBM and (b) the BOM. CB1 and CB2 are, respectively, the first and second conduction bands discussed in the text.

has a step-function-like threshold, as opposed to bulk silicon, which is known[23] to have a threshold depending on the photon energy $\hbar\omega$ as $(\hbar\omega - E_g)^{1/2}$, where E_g is the gap energy. Higher transition probabilities are thus expected in Si/SiO$_2$ SLs.

The numerical values of the various possible transition energies are given in Table I. For the DBM, the valence-band maximum is at the Γ point but the conduction-band minimum (CBM) is in between the Γ and X points (labeled $\Gamma X/2$ in Table I), giving an indirect gap of 0.81 eV. For the BOM, the VBM is at X while the CBM is at Z, giving an almost null (0.01 eV) indirect band gap. However, it should be remembered that the energy gaps are significantly underestimated in the LDA and other implementations of the DFT. Thus the bulk-Si LDA energy gap is 0.49 eV, about 0.6 eV below the true value of 1.1 eV, while the bulk-SiO$_2$ LDA energy gap (of the β-cristobalite phase, group $I\bar{4}2d$ with 144° Si-O-Si angles) is 5.78 eV, about 3.2 eV below the true value of 9 eV. Better (but certainly nonrigorous) estimates for the DBM energy gap would thus be restricted between 1.4 and 4.0 eV while for the BOM the energy gaps would remain between 0.6 and 3.2 eV. The unusually low value for the energy gap of the BOM is another indication that the lowest conduction band is really a gap state. Indeed, as indicated earlier, the

BOM contains only one bulklike Si layer (i.e., Si atoms having solely Si atoms as nearest neighbors), while the DBM has three. The band gap in the BOM should thus be significantly higher than in the DBM, as SiO$_2$ has a (much) larger gap than Si. Thus, if the first state in the BOM ["CB1" in Fig. 3(b)] is assumed to be an unphysical artifact of the model and temporarily ignored, the indirect gap (from VB to CB2) of 1.49 eV gets corrected to values between 2.1 eV and 4.7 eV, which is indeed beyond the band gap in the DBM. The energy gaps in both models would be in the visible part of the spectrum, consistent with experiment.[7,24,25]

The dispersionless character of the bands in the growth direction provides evidence of the confinement, as noted above. However, confinement alone is not sufficient to explain the enhancement of the optical properties; it is also determined by the atomistics of the interfaces, which must be taken into account explicitly. The optical enhancement in the two model structures will be considered in detail in Sec. III C, where we discuss our Fermi-golden-rule calculations of the optical transitions, which incorporate the effects of the dipole matrix element and the joint density of states. The joint density of states, which is provided by the band-structure calculations, is determined by the confinement of the bands as well as the modifications of the bands arising from interface-state effects. In a more qualitative sense, the direct or indirect nature of the bands provide immediate insight regarding the recombination of electron-hole pairs.

For the DBM, the direct transitions at Γ and $\Gamma X/2$ have energies of 0.98 eV and 0.84 eV, respectively, while the Γ-$\Gamma X/2$ indirect transition (i.e., the band gap) costs 0.81 eV. Thus the *smallest direct–indirect gap* (SDIG) in the LDA for the DBM is a mere 0.03 eV (0.84–0.81 eV). For the BOM (if the "CB1" gap state is, again, ignored), the direct transitions at X and Z have energies of 2.19 and 1.87 eV, respectively, compared to 1.49 eV for the Z-X indirect transition, for a SDIG of only 0.35 eV. These numbers can be compared to the corresponding ones for bulk silicon again in the *first* BZ (within the LDA): the direct transition at the Γ point has energy 2.52 eV while the direct transition at the CBM (near $3/4\Gamma X$) costs 3.20 eV. The indirect band gap is 0.49 eV, so that the SDIG in this case is ~2.0 eV. This is *much larger* than that for the DBM and the BOM. The latter, as a consequence, should have much better optical properties than bulk Si. It is also clear that the DBM will have better optical properties than the BOM (see Sec. III C) since the SDIG of the DBM is smaller than that of the BOM. Optical calculations will confirm these observations obtained from the electronic band structures.

B. Gap states in the BOM

In view of the presence of a gap state in the BOM — labeled "CB1" in Fig. 3(b) — and in order to assess the role of the interface on the electronic properties, other possibilities for the interfacial Si-O-Si angle were considered: (i) 109°, corresponding to positioning the oxygen atom on a normal silicon site of the Si lattice, here, $d_{\text{Si-O}} = 2.35$ Å ; (ii) 144° that corresponds to the experimental value of the Si-O-Si angle, used in the calculations discussed above, yield-
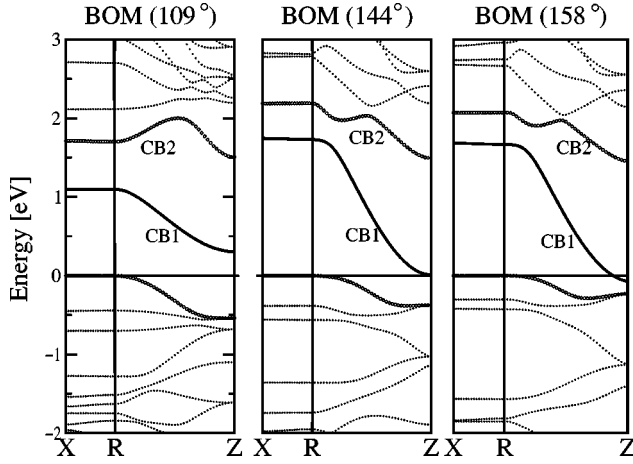
FIG. 4. Band structure of the BOM having three different interfacial Si-O-Si angles (as indicated).

ing $d_{\text{Si-O}} = 2.02$ Å; and finally (iii) 158°, a value obtained by relaxing the oxygen atom position, and which corresponds to a (local) energy minimum; in this case, $d_{\text{Si-O}} = 1.96$ Å. The "normal" Si-O distance in silica is 1.61 Å, which cannot be accomodated by the crystalline silicon lattice in the BOM.

Figure 4 shows the band structures for the three cases; here we consider only the X-R-Z direction, wherein lies the energy gap. Evidently, the precise value of the interfacial Si-O-Si bond angle, and corresponding Si-O bond length, have a sizeable effect on the band structure. In fact, the 158° BOM is, within the LDA, a metal if CB1 is not assumed to be a gap state, as discussed earlier. Likewise, the 144° BOM is nearly metallic. These results indicate that the acceptable range of interfacial Si-O-Si angles, and the consequently longer than "normal" Si-O distances, are probably essential issues in explaining the luminescence in Si/SiO$_2$ SLs.

In order to get a quantitative evaluation of the role of the CB1 energy level, we calculated the partial $1s$ core charge density of the interfacial oxygen atom in the BOM and compared it with the one of oxygen atoms inside the SiO$_2$ layer, at the CB1 and CB2 energy levels. This is done by summing the partial charge density over all the k points, and dividing it by the total (nuclear and electronic) charge of each nonequivalent oxygen atoms in the supercell, for the two energy levels considered. For the CB1 energy level, we find that the interfacial oxygen atom contributes 0.31% of the total core ($1s$) charge density, while oxygen atoms in the SiO$_2$ layer contribute only 0.04% of the total charge density. Now, the same calculation for the CB2 energy level gives 0.17% for the interfacial oxygen atom, while oxygen atoms in the SiO$_2$ layer contribute 0.137%. Thus, the ($1s$) charge density at CB1 is higher for the interfacial oxygen atom than for any oxygen atom in the SiO$_2$ layer, showing that the CB1 energy level and the interface oxygen atom are related. Structural relaxation of the interfacial oxygen atom would remove this spurious CB1 energy level; such calculations are in progress.

C. Optical properties

The Kohn-Sham calculations provide matrix elements and joint densities of states necessary for the calculation of the complex dielectric function $\vec{\epsilon} = \vec{\epsilon}_r + i\vec{\epsilon}_i$. The absorption coefficient α, which can then be deduced from $\vec{\epsilon}$ as a function of the photon energy (see below), provides a detailed picture of one aspect of the optical properties of the material. In principle, the luminescence requires a knowledge of the excited states of the system, with electrons occupying the conduction band. Such states are not available from DFT calculations. Further, the electrons in the conduction band are associated with holes in the valence band. For low-carrier concentrations, the screening is weak and hence exciton formation occurs.[26] This many-body effect is also required for a complete description of luminescence. Such calculations require, e.g., the solution of the Bethe-Salpeter equation for the electron-hole pair (see Chang Rohlfing, and Louie, Ref. 27) and are still prohibitive even for the simple-model structures considered here. Excitonic effects will thus be neglected here.

As already noted, the band gaps are underestimated by LDA-DFT and this has to be corrected if the absorption thresholds are to be realistic. In practice, this can be done to a reasonable approximation by rigidly shifting all the conduction bands to the appropriate energy. However, we remain within the DFT framework and calculate the absorption in the Fermi-golden-rule approximation. Also, we assume that the emission spectrum is similar to the absorption spectrum and neglect excitonic effects. In spite of these approximations, the main mechanisms of luminescence enhancement—the effects arising from the joint density of states and the matrix elements—would be correctly captured.

Using the program written by Abt, Ambrosch-Draxl, and Knoll[28] as part of the WIEN 97 package,[18] the imaginary part of the dielectric function has been determined, it is given by

$$\epsilon_i^\alpha(\omega) = \left(\frac{4\pi e^2}{m^2\omega^2}\right)\sum_{v,c}\int\frac{2d\vec{k}^3}{(2\pi)^3}|\langle c\vec{k}|\mathcal{H}^\alpha|v\vec{k}\rangle|^2 f_{v\vec{k}}(1$$
$$-f_{c\vec{k}})\delta(E_{c\vec{k}}-E_{v\vec{k}}-\hbar\omega),$$

where $f_{v\vec{k}}$ is the Fermi distribution and $\mathcal{H}^\alpha$ is the α component of the electron-radiation interaction Hamiltonian in the Coulomb gauge; it corresponds to the probability per unit volume for a transition of an electron in the valence-band state $|v\vec{k}\rangle$ to the conduction-band state $|c\vec{k}\rangle$ to occur. From Kramers-Kronig relations one then deduces the real part ϵ_r.[24] The dielectric function $\vec{\epsilon}$ is defined as the square of the complex refractive index $\vec{n} = n_r + in_i$, so that the absorption coefficient is given by

$$\alpha(E) = 4\pi\frac{E}{hc}n_i = 4\pi\frac{E}{hc}\left[\frac{(\epsilon_r^2+\epsilon_i^2)^{1/2}-\epsilon_r}{2}\right]^{1/2},$$

with c the speed of light in vacuum, h Planck's constant, and E the photon energy.

Figure 5 shows the z component of the absorption coefficients for the DBM and for the three different variations of the BOM. We also give, for comparison, the corresponding
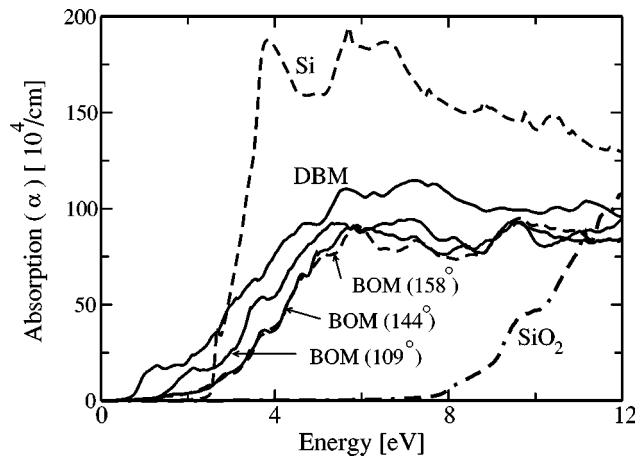
FIG. 5. Absorption curves for the two models compared to bulk Si and ideal β-cristobalite SiO_2. The three BOM angles correspond to the interfacial Si-O-Si angle in the model. The BOM curves for 144° and 158° overlap almost exactly; the full line corresponds to an angle of 144° while the dotted line corresponds to an angle of 158°.

curves for silicon and for the ideal β-cristobalite SiO_2 structures. The energy gaps are those ones directly from the LDA; correcting the gaps would only affect the position of the onset, but not the general aspect. The overall amplitude of the absorption coefficient for the two models are comparable. However, the onset of absorption occurs earlier in the DBM than in all variations of the BOM, correlating with the thickness of the bulklike Si layers—three atomic planes for the DBM vs one for the BOM. Our results thus confirm the shift towards the blue with increasing confinement observed in experiment.[7] Further, it is clear from Fig. 5 that the CB1 state in the BOM plays no role in the absorption, i.e., is *not* related to confinement; it is merely an artifact of the particular structure of the interface in this model.

Closer inspection of Fig. 5 reveals that the DBM has better-absorption properties than the three BOMs: the onset of absorption is sharper in the DBM, consistent with the band structure analysis above that showed the SDIG to be smaller in the DBM than in the BOM (~ 0.03 vs ~ 0.35 eV), and implying a larger transition probability for the former than the latter. Further, the interface suboxide Si atoms do have significant effects on the electronic and optical properties. For instance, the band gap (from VB to CB2) in the 109° BOM is 1.504 eV, while it is 1.493 eV and 1.451 eV for the 144° BOM and the 158° BOM, respectively. Such effects will be reconsidered within relaxed interface models.

Thus, the four models (the DBM and the BOM with bond angles 109°, 144° and 158°), which differ only by their interface definition, give rather different optical properties. The onset of the absorption curve in the BOM with Si-O-Si angles of 144° and 158° do not differ that much from the one obtained from bulk Si, while the DBM and the BOM with 109°, viz. the BOM with higher Si-O bond lengths at the interface, give better optical properties. This is additional indication that the interfacial atomic structure has to be connected to the optical enhancement in the SLs, in agreement with Kageshima's analysis.[16] Likewise, it can be concluded from Fig. 5 that bulk Si has poor optical properties compared to the SLs, since the onset of absorption lags behind that for the two SLs and the SDIG is much larger.

IV. CONCLUDING REMARKS

We have used first-principles calculations to (i) study the electronic and optical properties of Si/SiO_2 SL models and (ii) examine the applicability of tight-binding calculations for these systems.

Our calculations indicate that the band gap in both models is indirect (albeit quasi-direct), and in the visible region of the spectrum. Confinement is further demonstrated by the essentially dispersionless character of the electronic band structures in the growth direction (cf. Figs. 3). Our calculations show, also, that the SLs have enhanced optical properties as compared to pure Si.

The influence on the optical properties of the $Si-SiO_2$ interface has been assessed from calculations of the absorption coefficient. This quantity, we have shown, depends critically on the atomic details of the interfacial structure for a given ''state'' of confinement. Thus, realistic (interface) models are essential for determining completely the electronic and optical mechanisms in Si/SiO_2 SLs. We are presently examining such optimized structural models, with optical calculations going beyond those of Ref. 29.

*Author to whom correspondence should be addressed: Email address: laurent.lewis@umontreal.ca

[1] See various articles in *Proceedings of the 1998 International Conference on Applications on Photonic Technology III: Closing the Gap between Theory, Development, and Applications,* edited by G.A. Lampropoulos and R.A. Lessard (SPIE, Bellingham, 1998), Vol. 3491.

[2] P. Zhang, V.H. Crespi, E. Chang, S.G. Louie, and M.L. Cohen, Nature (London) **409**, 69 (2001).

[3] L.T. Canham, Appl. Phys. Lett. **57**, 1046 (1990).

[4] V. Lehmann and U. Gösele, Appl. Phys. Lett. **58**, 856 (1991).

[5] S.-F. Chuang, S.D. Collins, and R.L. Smith, Appl. Phys. Lett. **55**, 675 (1989).

[6] K. Uehara and J.S. Tse, Chem. Phys. Lett. **301**, 474 (1990).

[7] Z.H. Lu, D.J. Lockwood, and J.-M. Baribeau, Nature (London) **378**, 258 (1995).

[8] Z.H. Lu (private communication).

[9] F. Herman and I.P. Batra, in *The Physics of* SiO_2 *and its Inter-*

faces, edited by S.T. Pantelides (Pergamon, Oxford, 1978).

[10] N. Tit and M.W.C. Dharma-wardana, Phys. Lett. A **254**, 233 (1999).

[11] N. Tit and M.W.C. Dharma-wardana, J. Appl. Phys. **86**, 1 (1999).

[12] R. Williams, J. Vac. Sci. Technol. **14**, 1106 (1977).

[13] M.P.J. Punkkinen, T. Korhonen, K. Kokko, and I.J. Väyrynen, Phys. Status Solidi B **214**, R17 (1999).

[14] H. Kageshima and K. Shiraishi, in *Materials and Devices for Silicon-Based Optoelectronics*, edited by J.E. Cunningham, S. Coffa, A. Polman, and R. Soref, Mater. Res. Soc. Symp. Proc. No. **486** (Material Research Society, Pittsburgh, 1998), pp. 337.

[15] M.A. Herman and H. Sitter, *Molecular Beam Epitaxy* (Springer-Verlag, Berlin, 1989).

[16] Z.H. Lu, M.J. Graham, D.T. Jiang, and K.H. Tan, Appl. Phys. Lett. **63**, 2941 (1993).

[17] F.J. Himpsel, F.R. McFeely, A. Taleb-Ibrahimi, J.A. Yarmoff, and G. Hollinger, Phys. Rev. B **38**, 6084 (1988).

[18] P. Blaha, K. Schwarz, and J. Luitz, computer code WIEN 97 (Vienna University of Technology, Vienna, 1997) [Improved and updated UNIX version of the original copyrighted WIEN code, which was published by P. Blaha, K. Schwarz, P. Sorantin, and S.B. Trickey, Comput. Phys. Commun. **59**, 399 (1990)].

[19] D.J. Singh, *Planewaves, pseudopotentials and the LAPW method* (Kluwer Academic, Norwell, 1994).

[20] P. Hohenberg and W. Kohn, Phys. Rev. **136**, B864 (1964).

[21] W. Kohn and L.J. Sham, Phys. Rev. **140**, A1133 (1965).

[22] M.C. Payne, M.P. Teter, D.C. Allan, T.A. Arias, and J.D. Joannopoulos, Rev. Mod. Phys. **64**, 1045 (1992).

[23] P.Y. Yu and M. Cardona, *Fundamentals of Semiconductors* (Springer, New York, 1996).

[24] V. Mulloni, R. Chierchia, C. Mazzoleni, G. Pucker, L. Pavesi, and P. Bellutti, Philos. Mag. B **80**, 705 (2000).

[25] S.V. Novikov, J. Sinkkonen, O. Kilpelä, and S.V. Gastev, J. Vac. Sci. Technol. B **15**, 1471 (1997).

[26] R.S. Knox, *Solid State Physics* (Academic Press, New York, 1963).

[27] E.K. Chang, M. Rohlfing, and S.G. Louie, Phys. Rev. Lett. **85**, 2613 (2000).

[28] R. Abt, C. Ambrosch-Draxl, and P. Knoll, Physica B **194-196**, 1451 (1994).

[29] M. Tran, N. Tit, and M.W.C. Dharma-wardana, Appl. Phys. Lett. **75**, 4136 (1999).